Water Practice & Technology

IWA PUBLISHING

Water Practice & Technology Vol 16 No 4, 1397 doi: 10.2166/wpt.2021.074

Geophysical evaluation of geohydrokinetic properties of aquifer units in parts of Enugu state, Nigeria

Johnson Cletus Ibuot*, Emmanuel Tochukwu Omeje and Daniel Nnemeka Obiora

Department of Physics and Astronomy, University of Nigeria, Nsukka, Nigeria
*Corresponding author. E-mail: johnson.ibuot@unn.edu.ng

ABSTRACT

Vertical electrical sounding employing Schlumberger electrode configuration was carried out in thirty locations across some parts of Enugu state, to investigate the hydrokinetic properties of hydrogeologic units of the study area. The result shows that resistivity and thickness of aquifer ranges from 27.3 to 59,569.0 Ωm and 23.3 to 242.1 m respectively. Permeability and fractional porosity values range from 4,531.254 to 74,006.76 mD and 0.026 to 0.159. AQI having a mean value of 13.5451 μm range from 6.809 to 52.976 μm. FZI and HFU values range from 37.582 to 1,962.074 μm and 18 to 26 respectively. Contour maps were generated from the results to visualize the variations of the hydrokinetic properties across the study area. From the contour maps, the southern part of the study area was identified to be characterized with high AQI, FZI and HFU with the northwestern part and a small proportion along the southwestern part identified as areas with low AQI, FZI and HFU. HFU along the study area was observed to be fractionated into nine distinct properties (HFU 18, HFU 19, HFU 20, HFU 21, HFU 22, HFU 23, HFU 24, HFU 25, and HFU 26) with HFU 19 and HFU 20 dominating the area. The results from the nine hydraulic flow units based on flow zone indicator cut off values (Log FZI>0.25) show that the reservoir quality is very high.

Key words: aquifer, hydraulic, hydrokinetic, permeability, tortuosity

HIGHLIGHTS

- Groundwater repository was characterized using geohydrodynamic properties.
- The results revealed the dependency of AQI on tortuosity.
- The groundwater repository was classified into nine hydraulic flow units.
- The results show very high reservoir quality.
- The results revealed variations and interrelations of the parameters.

INTRODUCTION

Water is an essential demand of life and can be a great challenge when its extraction/exploitation is carried out without any geophysical knowledge about the area. Groundwater moves underground through the interconnected pores of rocks and soil, and stored in underground layers of water-bearing permeable rock, rock fractures or unconsolidated materials such as gravel, sand, or silt. Hydrofacies analysis of aquifer repositories can be employed to study the distribution of pore properties and aquifer quality. Complex variation comprehension in pore geometry having different lithofacies is a tool to advanced aquifer description and extraction. Aquifer architecture and quality is controlled by several factors, which include the hydrokinetic properties. Sedimentary facies and diagenesis control the porosity and permeability distribution in hydrogeologic units (Schlager 2005; George 2021). Groundwater, which is usually located within weathered, fractured or faulted chambers of rock units, has its occurrence, flow and storability in a rock terrain influenced by the geologic processes. As subsurface density increases, porosity decreases with depth due to pressure, which increases with depth (George *et al.* 2016). These geologic processes cause a change in the permeability, aquifer quality index, flow zone, and hydraulic flow unit, which are the hydrokinetic properties that act as dependent factors and indicators for the characterization and discharge of groundwater. Hydrokinetic properties are consistent properties that control fluid flow and enable segmenting of aquifers into different distinctive/unique geophysical classes. It also gives a distinction between geologic units having similar pore features. These distinctive properties tend to produce excellent aquifer characterization through classification of aquifer units into hydraulic flow units (George 2020). The knowledge of

permeability and porosity helps in understanding the hydrokinetic properties of hydrogeologic units. In groundwater repositories, the quality of groundwater is dependent on the efficiency of the flow unit and the contamination indices present in the unit (Abd-Elhamid & Javidi 2011; Basack *et al.* 2014; Ibuot & Obiora 2021). Accustomed examination and management of groundwater are extremely requisite as a result of possible contamination, which can be controlled by the hydrokinetic properties and geologic settings (Rao & Sreenivasulu 2004).

Electric resistivity method is a geophysical method that contributes significantly to groundwater exploration and exploitation, especially when pumping test is not affordable. Information realized from interpreted resistivity data gives a better understanding of the aquifer system. This work employed an indirect electrical resistivity technique in order to investigate and characterize the hydrokinetic properties of hydrogeologic units of sandy lithofacies.

LOCATION AND GEOLOGICAL SETTING OF THE STUDY AREA

The study area covers Nsukka, Igbo-Eze South and Udi local government areas of Enugu state and lies within the Anambra sedimentary basin in Nigeria. Nsukka and Igbo-Eze South span from 7°21′0′E to 7°32′0′E and 6°48′0′N to 7°2′0′N (Figure 1(a)) while Udi spans from 6°22′0′N to 6°26′0′N and 7°23′0′E to 7°26′0′E (Figure 1(b)). The study area is characterized by dry and wet seasons within the tropical rain forest/Guinea savannah belt of Nigeria. Nsukka Formation and the underlying Ajali Sandstone underlies the study area, the Ajali Sandstone is a thick friable, poorly sorted, and coarse-medium grained cross-bedded sandstone of Maastrichtian age (Omeje *et al.* 2021). Outcrops are seen in deep gullies incised along the lower slopes of an escarpment that run across the area from north to south separating two major drainage basins – the Cross river in the east and the Anambra on the west. Ajali Sandstone is underlain by the Mamu Formation (Lower Coal Measures) Campano-Maastrichtian age though outcrops of this formation are seen at the boundary of the Ajali Formation and

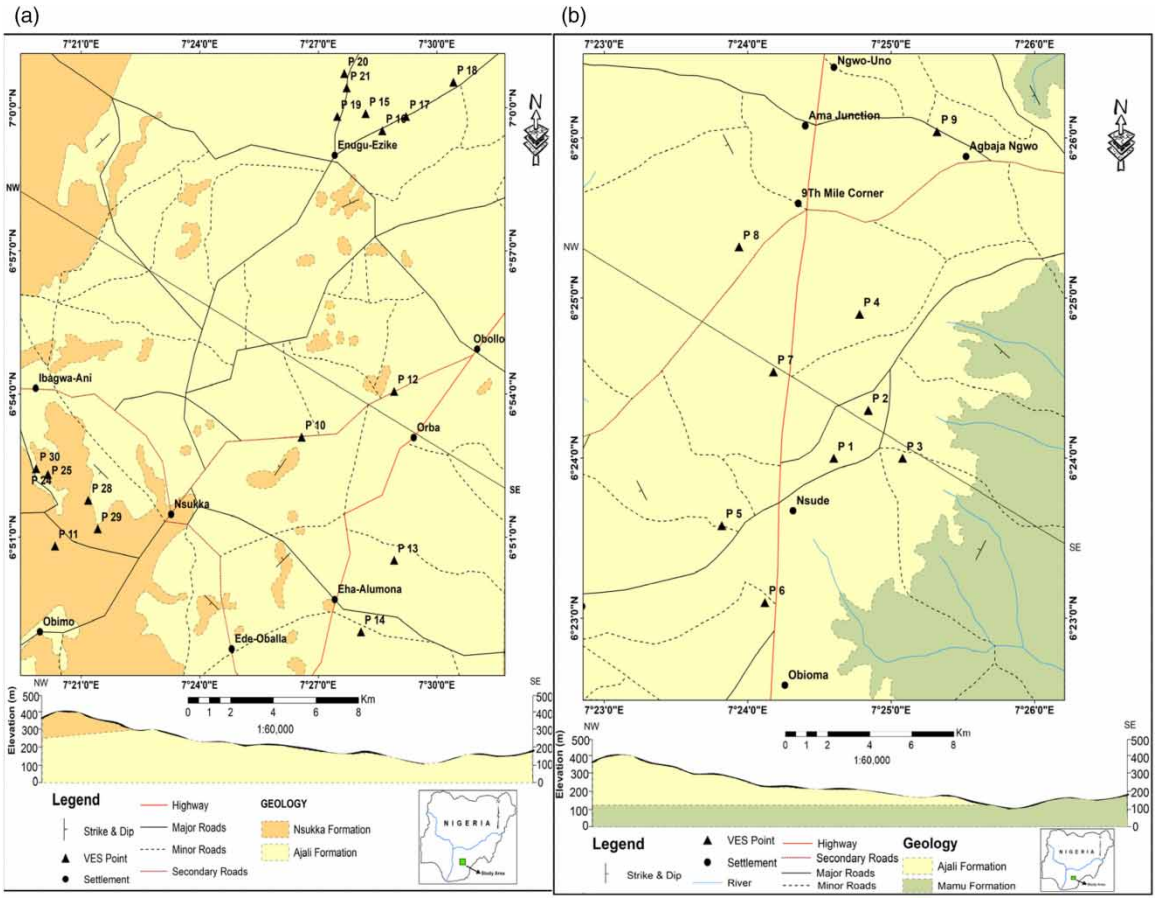

Figure 1 | Geologic map of the study areas: (a) Nsukka and Igbo-Eze South Local government areas, (b) Udi local government area.

Mamu Formation on the escarpment away from the study area. Also, the underlying Enugu shale is usually faced with seasonal fluctuations with little or no supply during the dry seasons as a result of the poor hydrologic nature of the shale. The shale group is massive and highly jointed with sets of vertical joints. It is generally not porous or permeable, but the formation could yield water to boreholes if fractured, the fractured nature makes it a potential aquifer repository. Also found in the study area are the residual hills and dry valleys, which are related to the rock type or geologic formation underlying the area (Stow 2005). Surface water body that traverse the area emanates from the contact between the bottom of the Ajali Formation and the upper part of the Mamu Formation at the foot of the scarp. Dry valleys and residual hills also characterize the study area as the prime landforms. These two major geomorphic structures are the resultant effect of weathering and differential erosion of clastic materials which are remnant of the Nsukka Formation. Figure 1.

MATERIALS AND METHODS

Estimating the hydrokinetic properties of different geologic units in the study area was achieved through the data acquired from thirty vertical electrical sounding points using a Schlumberger electrode configuration with the aid of 'SSR-MP-ATS' Resistivity Meter. Potential fields of current sent into the ground through one pair of electrodes each corresponding to potential and current electrode were measured. Extensible current electrode (AB) and potential electrode (MN) separation of 900 m and 40 m respectively were achieved by considering accessible roads in locating areas for VES points. For quality assurance in the field measurements, the separation between the potential electrodes was one fifth of the current electrode separations (George *et al.* 2016). MN varied from 0.5 m at AB = 2 m up to 40 m at AB = 900 m (Akpan *et al.* 2013). During field plating, two thirds of each electrode length perforated the subsurface. Apparent resistance (R_a) as measured from the field data were the vehicle to computing apparent resistivity (ρ_a) values shown in Equation (1):

$$\rho_a = \pi\left[\frac{\left(\frac{AB}{2}\right)^2 - \left(\frac{MN}{2}\right)^2}{MN}\right] R_a = K.Ra \tag{1}$$

where $\pi\left[\frac{\left(\frac{AB}{2}\right)^2 - \left(\frac{MN}{2}\right)^2}{MN}\right] = K$ is geometric factor, which depends on the electrode configuration.

Field data geologic model were obtained following Akpan *et al.* (2009). Plots of apparent resistivity against half current electrode spacing on a bi-logarithmic graph were carried out to achieve the manual modeling. Outliers at cross over points were deleted or readings averaged in order to extract lateral inhomogeneities from curves produced (Akpan *et al.* 2006; Chakravarthi *et al.* 2007). The bi-logarithmic graph was refined using a computer based VES modeling software program called WINRESIST, which generates geoelectric sounding curves in the process and classifies the curves into layers with different resistivity, depth and thickness (Figure 2).

In an attempt to identify the hydrokinetic properties (aquifer quality index, flow zone indicator and hydraulic flow unit) of the geologic units (*GU*) of the study area, hydrodynamic properties such as permeability, porosity and normalized porosity index were first estimated. Figure 3 illustrates a flow chart showing the research methodology.

Permeability values were estimated following the Kozeny (1927) and Carman (1939) generalized equation which was derived by the combination of Darcy's law for flow in a porous medium and Poiseuille's law for flow in a tube as shown in Equation (4).

$$Kp = \frac{\phi r}{8\tau^2} = \frac{\phi}{2\tau^2}\left(\frac{r}{2}\right)^2 = \frac{\phi r_m^2}{2\tau^2} \tag{2}$$

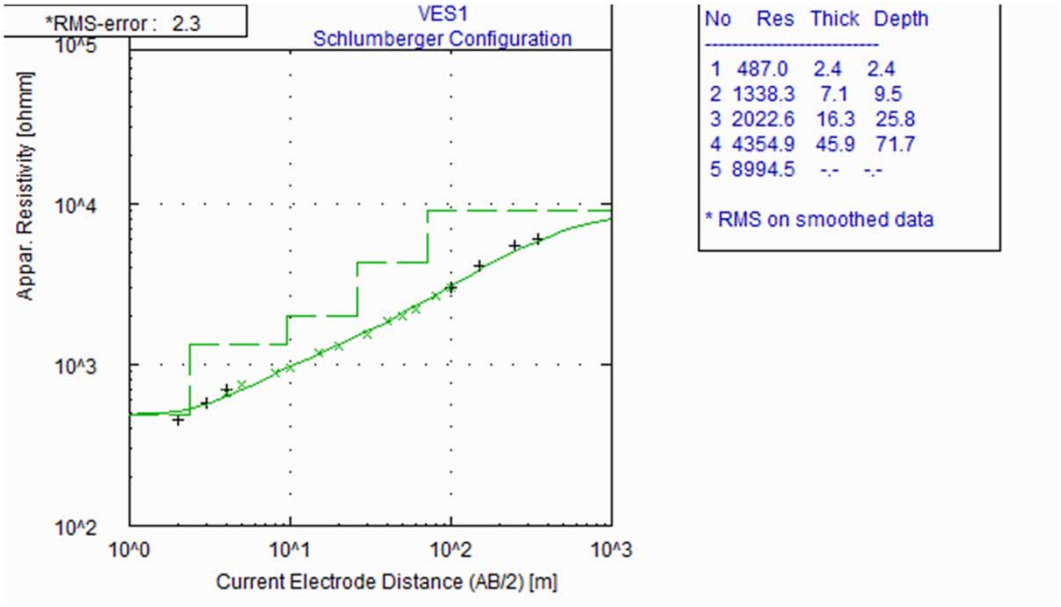

Figure 2 | VES curve showing VES1 resistivity, thickness and depth.

where Kp is in mD

$$S_{gv} = \frac{1}{r_m}\left(\frac{\phi}{1-\phi}\right) = \frac{1}{r_m} * PHIN \tag{3}$$

Combining Equations (2) and (3) produces the generalized Kozeny and Carmen equation in Equation (4).

$$Kp = \frac{\phi^3}{(1-\phi)^2}\left(\frac{1}{2\tau^2 S_{gv}^2}\right) = (PHIN)^2 * \phi * \left(\frac{1}{F_s \tau^2 S_{gv}^2}\right) \tag{4}$$

K is permeability, ϕ is effective fractional porosity, r_m is mean hydraulic radius, F_s is shape factor and it equals 2 for a circular cylinder, τ is tortuosity, $S_{gv}$is surface area per pore volume and $PHIN$ is the normalized porosity index. $F_s\tau^2 S_{gv}$ is a function of the geologic properties of the porous medium as it varies with changes in the pore geometry. Hydraulic conductivity (K_h) values were estimated following the Heigold *et al.* (1979) equation as shown in Equation (6).

$$K_h = \frac{386.40}{\rho a^{0.93283}} \tag{5}$$

where ρa is the aquifer resistivity in Ωm.

Porosity values of the GU of area were estimated with the knowledge of the water-bearing hydraulic conductivity of the area as shown in Equation (5).

$$\phi = 25.5 + 4.5 \ln K_h \tag{6}$$

Formation resistivity factor (F) and tortuosity values were estimated following Humbles equation and TNO (1976) equation, respectively, as shown in Equations (7) and (8):

$$F = \frac{0.62}{\phi^{2.15}} \tag{7}$$

$$\tau = \sqrt{F\phi} \tag{8}$$

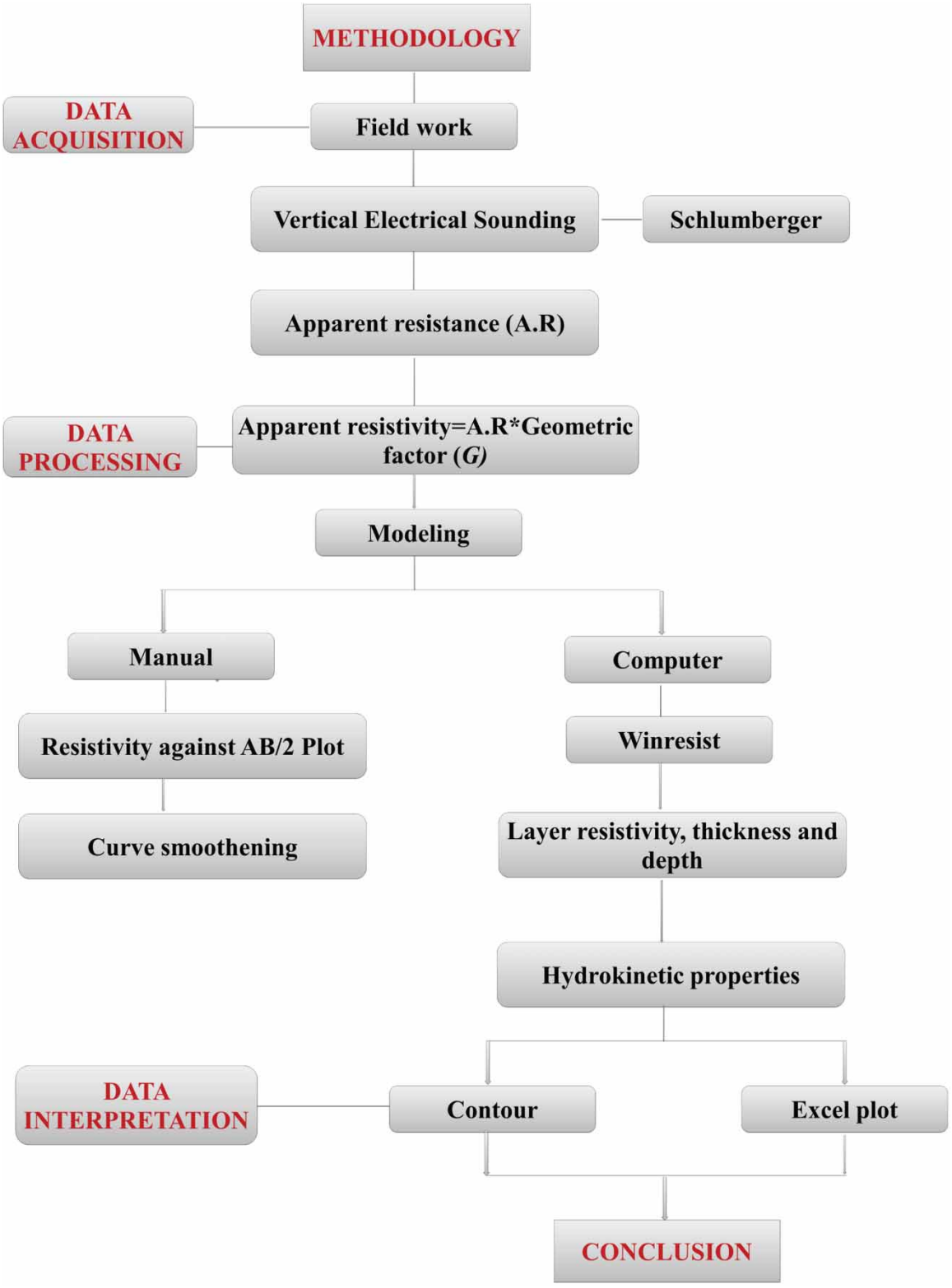

Figure 3 | Flow chart showing research methodology.

The hydraulic radius (r) values were estimated according to George *et al.* (2018) equation shown in Equation (9)

$$r = \sqrt{\frac{0.52 * \mu_d * K_h * \tau}{\delta_w * g * \phi}} \tag{9}$$

where μ_d is the dynamic viscosity of water which Fetters 1994 estimated as 0.0014 kg/ms and δ_w is the density of water which is 1,000 kg/m^3.

The aquifer quality index method presented a robust and reliable methodology for enhanced reservoir description which also captures the pore-body/throat attributes of a given aquifer system. The methodology, as introduced by Amaefule *et al.* (1993), is based on a modified Kozeny (1927) and Carman (1939) relationship. Each distinguished flow unit has a characteristic value of aquifer quality index. The aquifer quality index (AQI) concept is a unique and useful way to quantify the flow character of an aquifer through the use of the flow zone indicator (FZI).

$$AQI = \pi * 10^{-2} * \sqrt{\frac{K}{\phi}} \tag{10}$$

where AQI is in μm.

The FZI offers a relationship between geophysical properties on a large scale such as wellbore level. The flow zone indicator, which is controlled by the geophysical properties of the environment, was calculated using Equation (11):

$$FZI = \frac{AQI}{PHIN} \tag{11a}$$

where FZI is in μm.

AQI and FZI were employed to determine the API, which discriminates and specifies the rank of the aquifer potential. It is determined using Equation (11b):

$$API = \frac{AQI + FZI}{2} \tag{11b}$$

The flow zone model can be converted to 3D discrete rock type, which was employed in calculating the hydraulic flow (HFU) unit according to George (2020).

$$HFU = round[2 * \ln(FZI) + 10.6] \tag{12}$$

The key to a better aquifer characterization and exploitation emanates with the understanding of the differences in pore geometry within various lithofacies. These differences gave rise to a further subdivision known as flow units. A hydraulic flow unit according to Tiab & Donaldson (2004) is a continuous body over a specific aquifer volume that practically possesses consistent geophysical and fluid properties which uniquely characterize its static and dynamic communication with the wellbore. A hydraulic flow unit (HFU) is a representative volume or section of an aquifer. It can also be described as a section of the reservoir rock volume within which the pore throat characteristics of porous media regulating the fluid flow are unique and predictably different from the rest of the reservoir (Amaefule *et al.* 1993; Porras & Campos 2001). Each HFU, has a distinct geologic (sedimentary structure and texture) and geophysical (permeability and porosity) properties from properties of other section of the aquifer. Zonation of Hydraulic flow unit can be through Lorenz plot or the application of flow zone indicator. This work employed the FZI method as proposed by Amaefule *et al.* (1993) in determining the HFU of the aquifer in the study area.

RESULTS AND DISCUSION

The magnitude of the aquifer layer resistivity and thickness, as shown in Table 1, range from 27.3 to 59,569.0 Ωm and 23.3 to 242.1 m respectively. This range of values signifies the existence of low to high resistive geomaterial in the aquifer layer. Estimates of the hydrokinetic properties of the hydrogeologic units were obtained from this range of values. Spatial variability of these properties was visualized through graphs and contour maps. The variability of these properties is essential in prognosis of the dynamic characteristics of aquifers used in groundwater flow monitoring and management (Rao & Sreenivasulu 2004). Permeability (K_p) in $(\mu m)^2$ were changed to millidarcy (mD) by dividing K_p in $(\mu m)^2$ with a conversion factor given as 0.0009869233 $(\mu m)^2$ and the results

Table 1 | Summary of results of hydrokinetic properties of hydrogeologic units

VES Stations	Long. (^{O}E)	Lat. (^{O}N)	ρ_a(Ωm)	h_a(m)	K_h (m/day)	φ	PHIN	F	τ	API *(m)*	S_{gv} *(m^{-1})*	K_P (μm)^2	K_P *(mD)*	AQI (μm)	FZI (μm)	HFU
1	7.410	6.400	4,354.9	45.9	0.156	0.058	0.062	282.502	4.048	0.00089	1,123.222	5.392	5,463.444	9.637	155.435	21
2	7.414	6.405	9,954.7	104.7	0.072	0.073	0.079	172.285	3.546	0.000505	1,981.801	4.613	4,674.122	7.945	100.5700	20
3	7.418	6.400	11,336.2	58.1	0.064	0.076	0.082	157.995	3.465	0.000461	2,169.699	4.521	4,580.903	7.709	94.012	20
4	7.413	6.415	5,214.6	80.5	0.132	0.061	0.065	253.473	3.932	0.000787	1,270.59	5.163	5,231.41	9.195	141.462	21
5	7.397	6.393	5,495.6	72.8	0.125	0.062	0.066	244.765	3.896	0.000756	1,322.409	5.087	5,154.403	9.054	137.182	20
6	7.402	6.385	11,724.2	23.3	0.062	0.077	0.083	153.616	3.439	0.000449	2,227.244	4.521	4,580.903	7.659	92.277	20
7	7.403	6.409	20,445.6	134.4	0.037	0.094	0.104	100.038	3.067	0.000296	3,373.188	4.75	4,812.937	7.105	68.317	19
8	7.399	6.422	41,342.5	158.5	0.019	0.130	0.149	49.821	2.545	0.000165	6,076.945	6.033	6,112.937	6.809	45.698	18
9	7.422	6.434	27.3	24.0	17.674	0.026	0.027	1,585.620	6.421	0.017826	56.099	73.039	74,006.76	52.976	1,962.074	26
10	7.443	6.885	913.3	66.6	0.669	0.042	0.044	565.465	4.873	0.002377	420.676	9.675	9,803.193	15.170	344.773	22
11	7.339	6.847	230.9	73.9	2.412	0.034	0.035	890.660	5.503	0.005331	187.579	19.544	19,802.96	23.964	684.686	24
12	7.482	6.901	22,142.5	69.7	0.034	0.097	0.107	93.504	3.012	0.000277	3,607.059	4.704	4,766.328	6.960	65.047	19
13	7.482	6.842	59,569.0	242.1	0.014	0.159	0.189	32.314	2.267	0.000121	8,295.51	8.030	8,136.397	7.103	37.582	18
14	7.468	6.817	437.0	36.9	1.330	0.037	0.038	742.605	5.242	0.003704	269.998	13.336	13,512.7	18.976	499.368	23
15	7.47	6.998	12,226.0	181.7	0.059	0.078	0.085	149.413	3.414	0.000434	2,306.343	4.545	4,605.221	7.630	89.765	20
16	7.477	6.992	14,004.6	119.3	0.052	0.082	0.089	134.181	3.317	0.000391	2,555.447	4.52	4,579.89	7.421	83.382	19
17	7.487	6.997	7,528.1	93.9	0.093	0.068	0.073	200.677	3.694	0.000606	1,648.917	4.884	4,948.713	8.471	116.041	20
18	7.507	7.009	3,745.4	57.3	0.179	0.056	0.059	304.640	4.13	0.00098	1,020.063	5.492	5,564.769	9.898	167.763	21
19	7.458	6.997	14,180.5	140.3	0.052	0.082	0.089	134.181	3.317	0.000391	2,555.447	4.52	4,579.89	7.421	83.382	19
20	7.461	7.012	13,880.1	130.9	0.053	0.081	0.088	137.768	3.341	0.000399	2,506.69	4.472	4,531.254	7.427	84.398	19
21	7.462	7.007	1,836.4	63.6	0.349	0.048	0.050	424.349	4.513	0.001546	647.008	7.037	7,130.24	12.102	242.040	22
22	7.470	7.035	10,247.2	144.3	0.070	0.074	0.08	167.318	3.519	0.000492	2,031.382	4.634	4,695.4	7.9100	98.875	20
23	7.480	7.039	14,634.9	136.3	0.050	0.083	0.091	130.730	3.294	0.00038	2,631.035	4.575	4,635.619	7.421	81.549	19
24	7.331	6.874	25,777.5	107.4	0.030	0.103	0.115	82.185	2.909	0.000248	4,026.433	4.964	5,029.773	6.939	60.339	19
25	7.336	6.872	10,926.8	32.8	0.066	0.075	0.081	162.559	3.492	0.000473	2,114.248	4.514	4,573.81	7.754	95.728	20
26	7.677	6.630	36.3	29.0	13.549	0.027	0.028	1,462.041	6.283	0.01515	66.005	61.541	62,356.42	47.719	1,704.250	25
27	7.866	6.875	175.3	160.1	3.119	0.033	0.034	949.701	5.598	0.006206	161.127	23.444	23,754.63	26.641	783.559	24
28	7.353	6.863	360.3	112.3	1.593	0.036	0.037	787.665	5.325	0.004142	241.445	14.907	15,104.52	20.339	549.703	23
29	7.357	6.853	248.7	57.2	2.250	0.034	0.035	890.660	5.503	0.005149	194.215	18.231	18,472.56	23.145	661.286	24
30	7.331	6.874	10,480.5	30.3	0.069	0.074	0.080	167.318	3.519	0.000489	2,046.049	4.568	4,628.526	7.853	98.163	20

presented in Table 1. Porosity and permeability are key parameters that influence the flow in aquifer units and are spatially distributed across the study area. Figure 4 shows that a greater proportion of the southern parts of the study area are characterized with high permeability distribution having a range ≥40,000, with northern parts and a small fraction along the southwestern part characterized with low permeability distribution. Figure 5 shows the greater part of the study area as dominated with low porosity distribution having a range ≤0.05 with small portions in both the northwestern and southwestern part characterized with high porosity. This shows that greater parts of the southern zone, which are well permeable, are not highly porous and the northwestern parts, which are highly porous, are not well permeable, suggesting a poor interconnectivity of pores along the northwestern zone and the presence of clay in the aquifer. The discrepancy in pore system characteristics may be as a result of diagenetic and depositional characteristics (Jodeyri-Agaii *et al.* 2018). The high permeability distribution observed along the southern part of the study area despite low porosity can also be as a result of open and enlarged fractures in the geologic unit of the considered area. This explains the fact that porosity is not the only parameter upon which permeability variation can be explained. Due to high permeability in the southern zone, it can be deduced that the shale to sand ratio is appreciably low in the aquifer unit formation (George 2020).

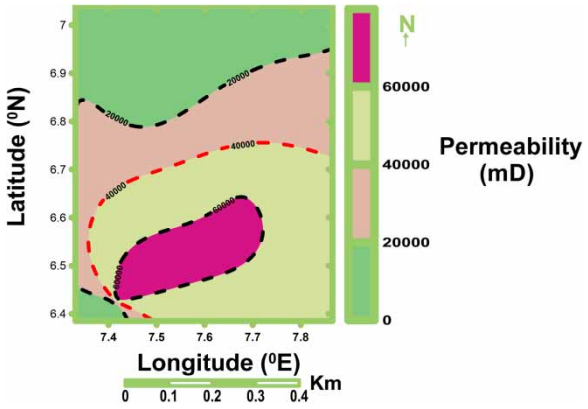

Figure 4 | Contour map showing permeability variation.

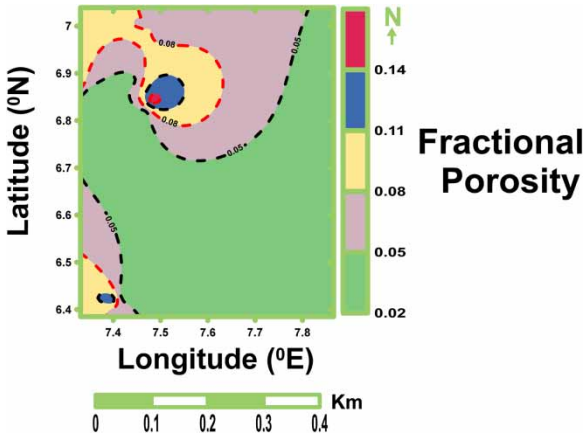

Figure 5 | Contour map showing fractional porosity variation.

Permeability variation can also be linked to the existence of more than one flow unit in an aquifer where each layer has distinct fluid flow properties. A fractional porosity-permeability relation for the study area was obtained as shown in Figure 6. Fractional porosity has an inverse functional power relation with permeability (in mD) having a coefficient of determination, $R^2 = 0.641$. Fractional porosity translation to permeability for groundwater reservoir in the study area is as given in Equation (13). The power relation in Equation (13) suggests that permeability (mD) in this study area is not wholly influenced by fractional porosity.

$$\phi = 4.109Kp^{-0.46} \tag{13}$$

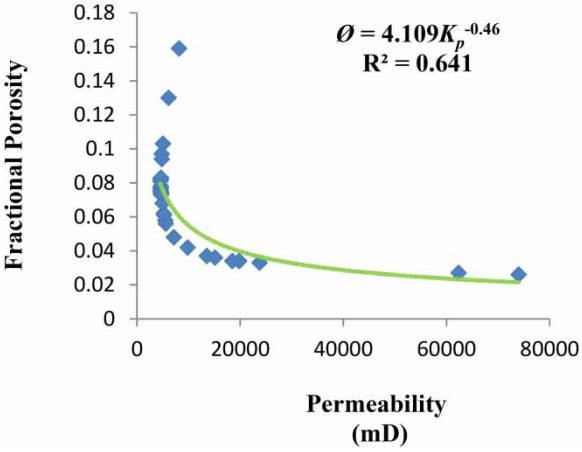

Figure 6 | Graph of porosity against permeability.

Tortuosity values range from 2.267 to 6.421, having an average value of 4.013. The greater part of the study area is characterized with high tortousity distribution ($\tau \geq 4.9$). The northwestern part and a small portion of the southwestern part are dominated with low tortuosity distribution as shown in Figure 7. This shows a possible difficulty in groundwater transmissibility along the southern and parts of the northeastern zones compared to other zones in the study area.

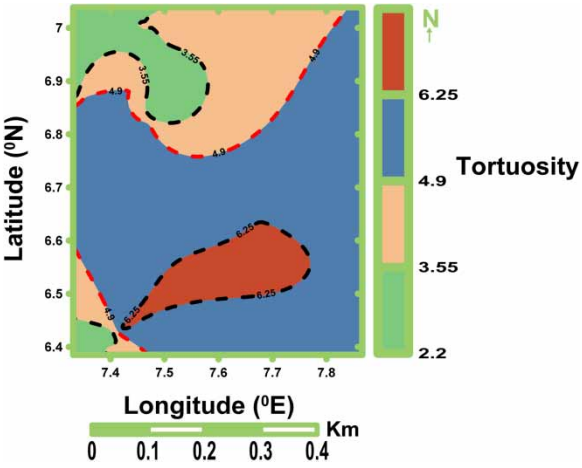

Figure 7 | Contour map showing tortuosity variation.

AQI ranges from 6.809 to 52.976 μm with an average value of 13.5451 μm. Figure 8 reveals a greater proportion of the southern part of the study area as characterized with high AQI (AQI ≥ 32) with the northern part and a small proportion of the southwestern part characterized with low AQI. The distribution of tortuosity and AQI in the study area shows similar variation, as regions of high AQI are associated with high tortuosities. This suggests that AQI of an area is affected by the nature of its tortuosity variation. The graph of AQI against tortuosity (Figure 9) reveals a direct polynomial relation, as shown in Equation (14), with a high coefficient of determination ($R^2 = 0.997$). The AQI, as acclaimed by Figure 9 and Equation (14), increases as tortuosity increases in an isotropic hydrogeologic unit.

$$AQI = 1.338\tau^3 - 12.99\tau^2 + 42.55\tau - 39.27 \quad (14)$$

FZI values range from 37.582 to 1,962.074 μm. From the value range, the study area is identified to be divided into high and low flow zones. Figure 10 shows the variation of FZI in the study area, having the northern and southern part of the study area characterized with low (FZI ≤ 1,100) and high (FZI ≥ 1,100) FZI respectively

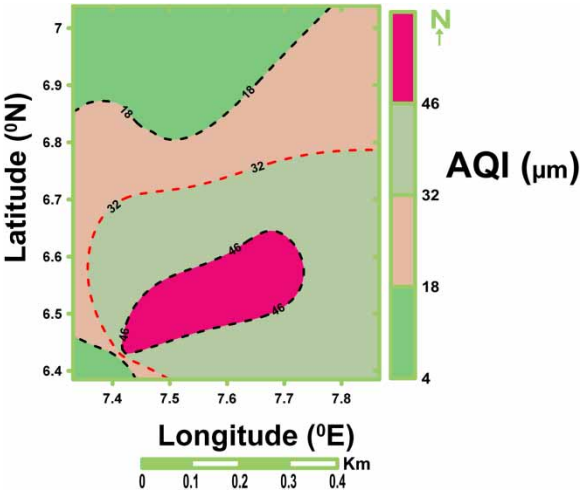

Figure 8 | Contour map showing AQI variation.

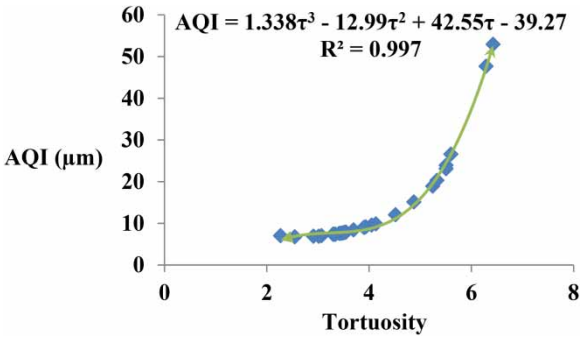

Figure 9 | Graph of AQI against tortuosity.

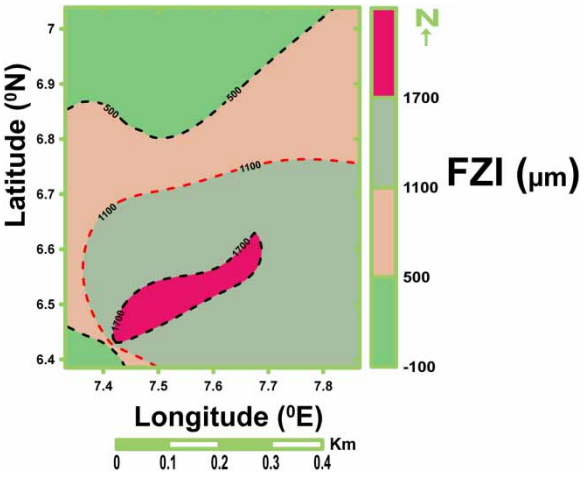

Figure 10 | Contour map showing FZI variation.

with a small portion in the southwestern part characterized with low FZI. From the variation, the aquifer layer in the northern part is characterized with pore filing and clays as well as fine grained poorly sorted sands, while the southern part is characterized with coarse grained and well-sorted sands (Kassab & Teama 2018).

Hydraulic flow unit variation from the contour map (Figure 11) shows its dependency on AQI and FZI as its variation reveals its similarity with AQI and FZI. The similarity in the distribution shows the manifestation of the

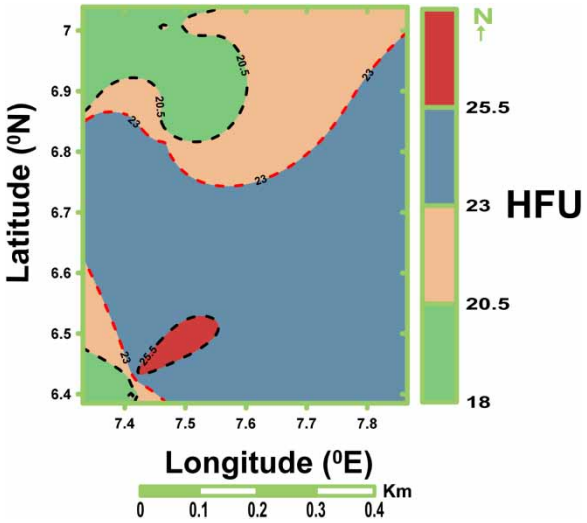

Figure 11 | Contour map showing HFU variation.

distinctiveness of the hydraulic unit in the considered parameters. Table 1 shows that HFU values range from 18 to 26. Figure 11 shows the greater part of the study area as characterized with high hydraulic flow unit (HFU $\geq$ 23), with the northern part and a small portion along the southwestern part characterized with low HFU (HFU $\leq$ 23). HFU along the study area is divided into nine distinct properties (18, 19, 20, 21, 22, 23, 24, 25 and 26). These properties differ from one unit to another but are similar in the same flow unit. This reflects the fact that each unit has fluid flow properties different from other units.

Figure 12 shows classification of thirsty hydrogeologic units on the basis of a quantum geologic formation also referred to as a hydraulic unit. From the hydrogeologic units identified, nine locations show similar hydraulic units sticking to 20, three locations show hydraulic units conforming to 18, 22 and 23 respectively, seven locations with HU sticking to 19, two locations with HU sticking to 21 and 24, while one location each has HU conforming to 25 and 26. From Figure 12, it is observed that a greater number of hydrogeologic unit locations conform to HU 20 and HU 19. Following Jodeyri-Agaii *et al.* (2018), the reservoir quality of the nine hydraulic flow units observed in the considered hydrogeologic unit is very high based on cut-off values on the flow zone indicator (Log FZI>0.25). The illustration in Figure 12 suggests that sediments, with similar fluid flows should be mapped out and grouped together (Gholinezhad & Masihi 2012).

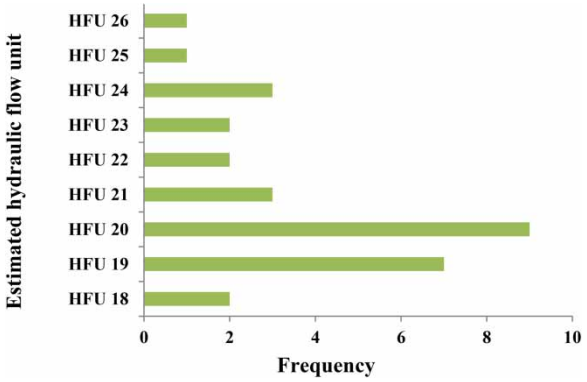

Figure 12 | Graph showing estimated hydraulic flow units and its frequency.

The relation between HFU and FZI as shown in Figure 13 and Equation (15) reveals a proportion curved line and direct relation between the two properties. The relation shows that an increasing FZI will result in an increasing hydraulic flow unit within a homogenous aquifer unit. This may not be applicable in a heterogeneous unit as a distinctive hydraulic unit will not uphold to the FZI attributed outside its vault (George *et al.* 2017). Formations

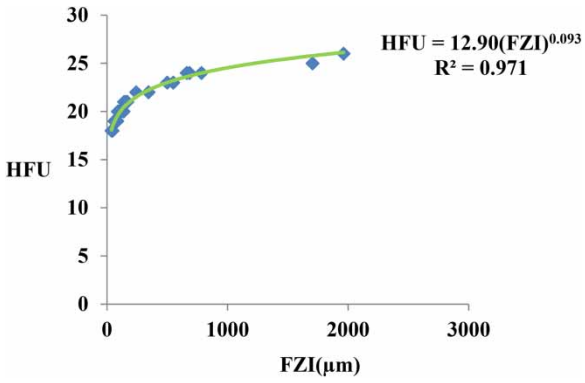

Figure 13 | Graph of hydraulic flow unit against flow zone Indicator.

with a narrow range of flow zone indicator magnitude belong to an innate hydraulic flow unit (Prasad 2003).

$$HFU = 12.90(FZI)^{0.093} \quad (15)$$

CONCLUSION

Electrical resistivity results have been used to estimate the hydrokinetic properties of hydrogeologic units of some parts of Enugu state. The results reveal the distribution and inter-relationship of these properties in the considered units. The result shows that permeability of the hydrogeologic unit is not wholly dependent on the unit's fractional porosity, as southern parts of the study area, which are highly permeable, are not highly porous. The result reveals the dependency of AQI on tortuosity as areas with high AQI correspond to areas with high tortuosity. Hydrokinetic properties are a bona fide tool for flow unit estimation and characterization of groundwater repository into their specific hydraulic units based on quantum geologic formation type. The result of the hydrokinetic properties reveals that VES stations established at the southern part of the study area account for areas with high tortuosity, AQI, FZI and HFU with the northwestern part and a small fraction on the southwestern part characterized with low tortuosity, AQI, FZI and HFU. The hydrogeologic unit of the study area was observed to be classified into nine hydraulic flow units (HFU 18, HFU 19, HFU 20, HFU 21, HFU 22, HFU 23, HFU 24, HFU 25 and HFU 26) with HFU 19 and HFU 20 dominating the study area. The results from the nine hydraulic flow units based on flow zone indicator cut-off values (Log FZI>0.25) show that the reservoir quality is very high. The empirical relations connecting the hydrokinetic properties were generated and the equations derived could be applied in modeling groundwater repositories for productive characterization of groundwater into its unique hydraulic units.

ACKNOWLEDGEMENT

The authors are grateful to the atmospheric and geophysics research group in the department of Physics and Astronomy, University of Nigeria, Nsukka.

DECLARATION OF COMPETING INTEREST

The authors declare no conflicts of interest.

DATA AVAILABILITY STATEMENT

All relevant data are included in the paper or its Supplementary Information.

REFERENCES

Abd-Elhamid, H. F. & Javidi, A. A. 2011 A cost-effective method to control seawater intrusion in coastal aquifers. *Water Resource Management* **25**(11), 2755–2780. doi: 10.1007/s11269-011-9837-7.

Akpan, F. S., Etim, O. N. & Akpan, A. E. 2006 Geoelectrical investigation of groundwater potential in parts of Etim Ekpo local government area, Akwa Ibom State. *Nigerian Journal of Physics* **18**, 39–44. doi:10.4314/njphy.v18i1.38080.

Akpan, A. E., George, N. J. & George, A. M. 2009 Geophysical investigation of some prominent gully erosion sites in Calabar, south-eastern Nigeria and its implications to hazard prevention. *Disaster Adv* **2**(3), 46–50.

Akpan, A. E., Ugbaja, A. N. & George, N. J. 2013 Integrated geophysical, geochemical and hydrogeological investigation of shallow groundwater resources in parts of the Ikom- Mamfe Embayment and the adjoining areas in Cross River State, Nigeria. *Environmental Earth Sciences* **70**(3), 1435–1456. doi: 10.1007/s12665-013-2232-3.

Amaefule, J. O., Altunbay, M., Tiab, D., Kersey, D. G. & Keelan, D. K. 1993 Enhanced reservoir description using core and log data to identify hydraulic (flow) and predict permeability in uncored intervals/wells. In: *SPE 26436, Presented at 68th Annual Technical Conference and Exhibition*, Houston, Texas. https://doi.org/10.2118/26436-MS

Basack, S., Bhattacharya, A. K. & Maity, P. 2014 A coastal groundwater management model with Indian case study. *Proceedings of the Institution of Civil Engineers: Water Management* **167**(3), 126–140. https://doi.org/10.1680/wama.12.00008.

Carman, P. C. 1939 Permeability of saturated sands, soils and clays. *Journal of Agricultural Science* **29**, 263–273. https://doi.org/10.1017/S0021859600051789.

Chakravarthi, V., Shankar, G. B. K., Muralidharan, D., Harinarayana, T. & Sundararajan, N. 2007 An integrated geophysical approach for imaging subbasalt sedimentary basins: case study of Jam river basin, India. *Geophysics* **72**(6), 141–147. https://doi.org/10.1190/1.2777004.

Fetters, C. W. 1994 Applied hydrogeology, 3rd edn. Prentice Hall, Englewood Cliffs, New Jersey, p 600.

George, N. J. 2020 Appraisal of hydraulic flow units and factors of the dynamics and contamination of hydrogeological units in the littoral zones: a case study of Akwa Ibom State University and its Environs, Mkpat Enin L.G.A, Nigeria. *Journal of the International Association for Mathematical Geosciences*. doi: 10.1007/s11053-020-09673-9.

George, N. J. 2021 Geo-electrically and hydrogeologically derived vulnerability assessments of aquifer resources in the hinterland of parts of Akwa Ibom State, Nigeria. *Solid Earth Sciences* **6**(2), 70–79. doi:10.1016/j.sesci.2021.04.002.

George, N. J., Akpan, A. E. & Ekanem, A. M. 2016 Assessment of textural variational pattern and electrical conduction of economic and accessible quaternary hydrolithofacies via geoelectric and laboratory methods in SE Nigeria: a case study of select locations in Akwa Ibom State. *Journal of Geological Society of India* **88**(4), 517–528. doi:10.1007/s12594-016-0514-6.

George, N. J., Ekanem, A. M., Ibanga, J. I. & Udosen, N. I. 2017 Hydrodynamic implications of Aquifer Quality Index (AQI) and Flow Zone Indicator (FZI) in groundwater abstraction: a case study of coastal hydro-lithofacies in south-eastern Nigeria. *Journal of Coastal Conservation* **21**, 759–776. https://doi.org/10.1007/s11852-017-0535-3.

George, N. J., Ibuot, J. C., Ekanem, A. M. & George, A. M. 2018 Estimating the indices of intertransmissibility magnitude of active surficial hydrogeologic units in Itu, Akwa Ibom State, southern Nigeria. *Arabian Journal of Geoscience* **11**, 1–16. doi 10.1007/s12517-018-3475-9.

Gholinezhad, S. & Masihi, M. 2012 A physical-based model of permeability/porosity relationship for the rock data of Iran southern carbonate reservoirs. *Iranian Journal of Oil and Gas Science and Technology* **1**(1), 25–36. doi:10.22050/IJOGST.2012.2772.

Heigold, P. C., Gilkeson, R. H., Cartwright, K. & Reed, P. C. 1979 Aquifer transmissivity from surficial electrical methods. *Groundwater* **17**(4), 338–345. doi.org/10.1111/j.1745-6584.1979.tb03326.x.

Ibuot, J. C. & Obiora, D. N. 2021 Estimating geohydrodynamic parameters and their implications on aquifer repositories: a case study of University of Nigeria, Nsukka, Enugu State. *Water Practice and Technology* **I6**(1), 162–181.

Jodeyri-Agaii, R., Rahimpour-Bonab, H., Tavakoli1, V., Kadkhodaie-Ilkhchi, R. & Yousefpour, M. R. 2018 Integrated approach for zonation of a mid-Cenomanian carbonate reservoir in a sequence stratigraphic framework. *Geologica Acta* **16**(3), 321–337. doi: 10.1344/GeologicaActa2018.16.3.5. https://doi.org/10.1344/GeologicalActa2018.16.3.5.

Kassab, M. A. & Teama, M. A. 2018 Hydraulic flow unit and facies analysis integrated study for reservoir characterisation: a case study of Middle Jurassic rocks at Khashm El-Galala, Gulf of Suez, Egypt Arabian. *Journal of Geosciences* **11**, 294. https://doi.org/10.1007/s12517-018-3595-2.

Kozeny, J. 1927 Ueber kapillare leitung des wassers im boden: Sitzungsberichte der. *Akademie der Wissenschaften in Wien* **136**, 271–306.

Omeje, E. T., Ugbor, D. O., Ibuot, J. C. & Obiora, D. N. 2021 Assessment groundwater repositories in Edem, Southern Nigeria, using vertical electrical sounding. *Arabian Journal of Geosciences* **14**, 42.

Porras, J. C. & Campos, O. 2001 Rock typing: a key approach for petrophysical characterization and definition of flow units, Santa Barbara Field, Eastern Venezuela Basin. In: *Society of Petroleum Engineers. (SPE), Buenos Aires (Argentina), Latin American and Caribbean Petroleum Engineering Conference*, 25–28 March. p. 6. https://doi.org/10.2118/69458-MS

Prasad, M. 2003 Velocity–permeability relations within hydraulic units. *Geophysics* **68**, 108–117. https://doi.org/10.1190/1.1543198.

Rao, S. V. N. & Sreenivasulu, V. 2004 Planning groundwater development in coastal aquifers. *Hydrological Science* **49**(1), 155–170. https://doi.org/10.1623/hysj.49.1.155.53999.

Schlager, W. 2005 Carbonate sedimentology and sequence stratigraphy. *SEPM, Concepts in Sedimentology and Paleontology*. Series 8, p. 200. https://doi.org/10.2110/csp.05.08.

Stow, D. A. V. 2005 *Sedimentary Rocks in the Field: A Colour Guide*. Mason Publ. Ltd, London, p. 320.

The Netherland Organization 1976 Geophysical well logging for geohydrological purposes in unconsolidated formations. Groundwater Survey TNO. The Netherlands Organization for Applied Scientific Research, Delft. OCLC no: 68104428.

Tiab, D. & Donaldson, E. C. 2004 *Petrophysics*. Elsevier, Amsterdam, p. 105.

First received 19 April 2021; accepted in revised form 21 July 2021. Available online 4 August 2021